

LARGE DEFLECTION ANALYSIS OF A  
CIRCULAR PLATE WITH A CONCENTRICALLY  
SUPPORTING OVERHANG

By

Ibrahim Abdul-Jabbar Zabad

---

A Thesis Submitted to the Faculty of the  
DEPARTMENT OF CIVIL ENGINEERING AND ENGINEERING MECHANICS

In Partial Fulfillment of the Requirements  
For the Degree of

MASTER OF SCIENCE  
WITH A MAJOR IN CIVIL ENGINEERING

In the Graduate College

THE UNIVERSITY OF ARIZONA

1 9 8 1

STATEMENT BY AUTHOR

This thesis has been submitted in partial fulfillment of requirements for an advanced degree at The University of Arizona and is deposited in the University Library to be made available to borrowers under rules of the Library.

Brief quotations from this thesis are allowable without special permission provided that accurate acknowledgment of source is made. Requests for permission for extended quotation from or reproduction of this manuscript in whole or in part may be granted by the head of the major department or the Dean of the Graduate College when in his judgment the proposed use of the material is in the interests of scholarship. In all other instances, however, permission must be obtained from the author.

SIGNED: \_\_\_\_\_

*Randall Zassari*

APPROVAL BY THESIS DIRECTOR

This thesis has been approved on the date shown below:

*D. Dadeppo*  
\_\_\_\_\_  
D. DADEPPO  
Professor of Civil Engineering

*April 17, 1981*  
\_\_\_\_\_  
Date

## ACKNOWLEDGMENTS

I would like to express my appreciation and gratitude to Professor Donald A. DaDeppo for his guidance and for his intelligent lectures that provided the necessary background for the development of this thesis.

I would like to extend my appreciation to Dean Richard H. Gallagher for his endurance and understanding during the course of my study.

Special thanks and appreciation to Dr. Ibrahim Almadhoun and Dr. Riyad Qashu for their assistance, and to Thomas A. Ladd and David R. Pettijohn.

Finally, sincere gratitude and appreciation are due to my father whose moral and financial support and inexhaustible patience have made this possible.

## TABLE OF CONTENTS

	Page
LIST OF FIGURES . . . . .	v
ABSTRACT . . . . .	vi
NOMENCLATURE . . . . .	vii
CHAPTER	
1 INTRODUCTION . . . . .	1
2 CIRCULAR PLATE EQUATIONS . . . . .	3
3 BOUNDARY CONDITIONS . . . . .	6
4 NUMERICAL PROCEDURE . . . . .	8
Determination of the Partial's . . . . .	12
Determination of Good Estimates for $w_1$ , $M_{r1}$ , and $N_{r1}$ . . . . .	14
5 PRESENTATION AND DISCUSSION OF RESULTS . . . . .	15
6 CONCLUSION . . . . .	21
REFERENCES . . . . .	22

## LIST OF ILLUSTRATIONS

Figure		Page
2.1	Geometry of the plate . . . . .	3
2.2	Stresses on a plate element . . . . .	4
2.3	Circular section of radius $r$ . . . . .	5
3.1	Plate section at the support . . . . .	7
4.1	Section of the plate showing the boundaries .	9
5.1	Results obtained by both perturbation method and the method described in this study . . . . .	16
5.2	The deflections at the center of the plate versus the load, for different values of $\alpha$ . . . . .	19
5.3	Stress versus load . . . . .	20

## ABSTRACT

This thesis concerns the application of numerical techniques for the non-linear analysis of a uniformly loaded circular plate with an overhang, and simply supported on a concentric circle. The numerical technique involves an iterative process which employs the fourth-order Runge-Kutta integration scheme and Newton-Raphson root-finding method.

## NOMENCLATURE

- $a$  = radius of the plate
- $b$  = radius of the support
- $D$  = flexural rigidity of the plate:  $Eh^3/12(1 - \nu^2)$
- $E$  = modulus of elasticity in tension and compression
- $M_r$  = radial moment
- $M_t$  = tangential moment
- $N_r$  = normal force per unit length in the radial direction
- $N_t$  = normal force per unit length in the tangential direction
- $Q$  = shearing force in the radial direction per unit circumferential length
- $R_s$  = support reaction
- $q_1, q_2$  = uniform load within the support circle and along the overhang, respectively
- $r$  = radius
- $u$  = radial component of the displacement of a point in the middle plane of the plate
- $w$  = vertical deflection, positive downward
- $w_0$  = vertical deflection at the center of the plate
- $\phi$  = angular displacement

$\lambda$  = load parameter

$\nu$  = Poisson's ratio

$\sigma_r$  = radial stress

$\sigma_t$  = tangential stress



## CHAPTER 1

### INTRODUCTION

In restricting the analysis of a thin circular plate to a small deflection-small rotation theory, the membrane action (i.e., membrane stresses and extension of the middle plane) can be neglected. The problem then reduces to solving a relatively simple linear fourth-order differential equation.

However, when the deflection becomes about half the thickness of the plate and higher, the plate takes on a non-developable surface (Timoshenko and Woinowsky-Krieger, 1959), and the membrane action can no longer be ignored. Hence the large-deflection problem resolves itself into solving two second-order, simultaneous nonlinear differential equations (so-called von Karman equations).

In the investigation that follows, we consider the large-deflection analysis of a circular plate with an overhang. This plate is simply supported on a concentric circle, and axisymmetrically loaded. The loading is uniform and can be applied within the support circle, the overhang, or any combination of both.

A particular case, when the uniform load is within the support circle, was solved by Lee, Lim and Conway (1980) using a perturbation method developed by Vei-Chan and Kai-Yoan.

The objective of this thesis, however, is to obtain more accurate results, and solutions for a wider range of loading. This was done by utilizing the Newton-Raphson method in conjunction with numerical integration.

## CHAPTER 2

### CIRCULAR PLATE EQUATIONS

The bending properties of a plate depend greatly on the radius-to-thickness ratio. In the case when the ratio is relatively low the problem becomes more involved and must be analyzed as a three-dimensional elasticity problem. This research, however, was restricted to obtaining a solution for relatively thin circular plates with large deformations. These deformations are small enough that third- and higher-order non-linearities may be neglected.

The geometry of the problem is shown in Figure 2.1.

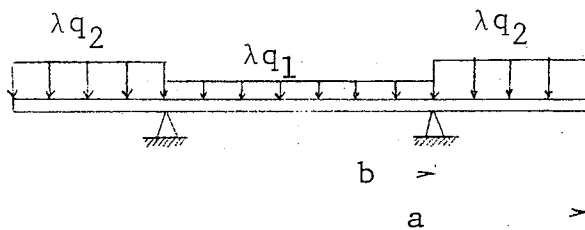


Figure 2.1. Geometry of the plate.

Referring to Timoshenko and Woinowsky-Krieger (1959) the governing equations for plates with large deflections are (see Figure 2.2):

$$\frac{du}{dr} = \frac{1}{Eh} (N_r - \nu N_t) - 1/2 \phi^2 \quad (2.1a)$$

$$\frac{d}{dr} (r\phi) = \frac{r}{(1+\nu)D} (M_r + M_t) \quad (2.1b)$$

$$\frac{dw}{dr} = -\phi \quad (2.1c)$$

$$\frac{d}{dr} (rM_r) = M_t - Qr \quad (2.1d)$$

$$\frac{d}{dr} (rN_r) = N_r \quad (2.1e)$$

$$N_t = Eh \frac{u}{r} + \nu N_r \quad (2.1f)$$

$$M_t = \nu M_r + (1-\nu^2)D \frac{\phi}{r} \quad (2.1g)$$

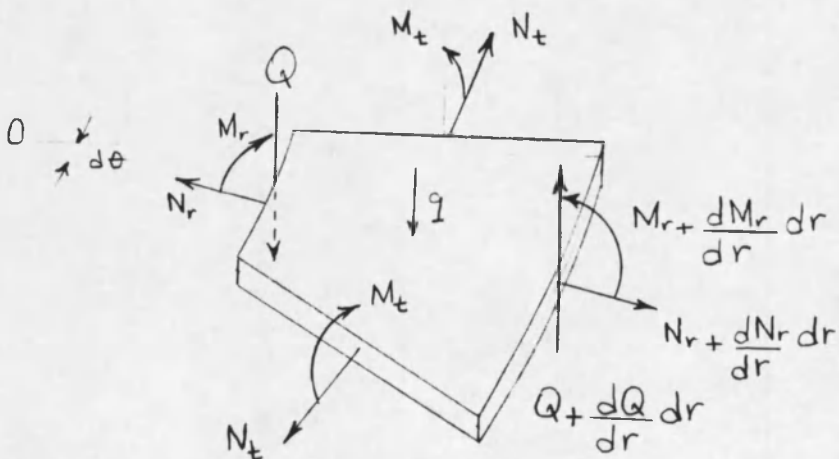


Figure 2.2. Stresses on a plate element.

From Figure 2.3, equilibrium in the vertical direction yields:

$$Q = -N_r \phi + \frac{\lambda q_1}{2} r \quad \text{for } 0 < r < b$$

$$Q = -N_r \phi - \frac{\lambda q_2}{2r} (a^2 - r^2) \quad \text{for } b < r < a$$

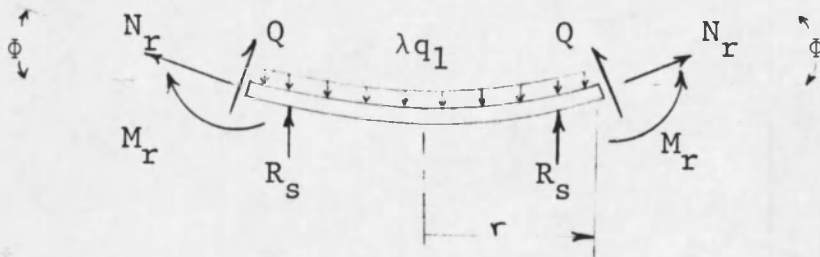


Figure 2.3. Circular section of radius  $r$ .

## CHAPTER 3

### BOUNDARY CONDITIONS

Since the plate is axisymmetrically loaded (Figure 2.1), the axis of the plate is an axis of symmetry. Hence it can be deduced that the radial component of the displacement of the middle plane of the plate at the center is zero and also the slope.

$$u(r = 0) = 0 \quad (3.1)$$

$$\phi(r = 0) = 0 \quad (3.2)$$

The radial component of the displacement of the middle plane of the plate, the angular deformation, and the radial moment are continuous to the left and right of the support (Figure 2.1). The deflection is also continuous at the support and has a zero value. Therefore:

$$w(r = b^-) = w(r = b^+) \quad (3.3)$$

$$w(r = b) = 0 \quad (3.4)$$

$$u(r = b^-) = u(r = b^+) \quad (3.5)$$

$$\phi(r = b^-) = \phi(r = b^+) \quad (3.6)$$

$$M_r(r = b^-) = M_r(r = b^+) \quad (3.7)$$

From Figure 3.1, equilibrium along the direction of the radial stress yields (see Figure 3.1):

$$N_r(r=b^+) = N_r(r=b^-) + \frac{\lambda\phi}{2b} [q_1 b^2 + q_2 (a^2 - b^2)] \quad (3.8)$$

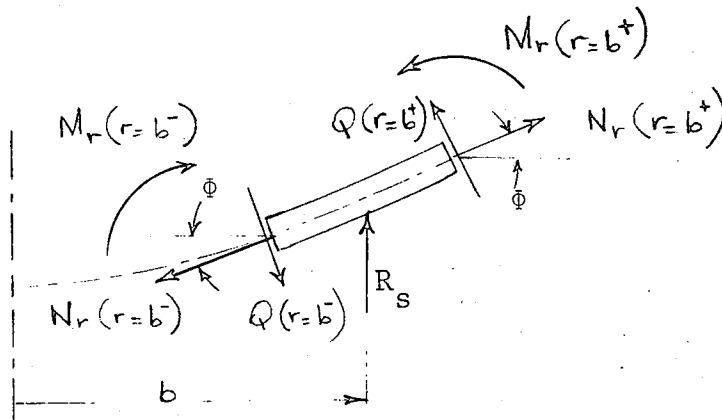


Figure 3.1. Plate section at the support.

Finally, at the edge of the plate the radial moment and the radial stress are zero.

$$M_r(r = a) = 0 \quad (3.9)$$

$$N_r(r = a) = 0$$

## CHAPTER 4

### NUMERICAL PROCEDURE

After a careful study of the circular plate equations in Chapter 2, it can be deduced that the plate problem resolves itself into solving a set of five simultaneous non-linear differential equations. Closed-form analytical solutions for the plate problem are very difficult, if not impossible, to obtain. However, this research resorts to a numerical method which treats the problem as a three-point boundary value problem. These boundaries are the center of the plate, the support, and the edge of the plate. This numerical method involves Kutta's Simpson's rule in conjunction with Newton-Raphson root-finding scheme. It starts by assuming trial values for the unknown field variables at the center of the plate (i.e.,  $w$ ,  $M_r$  and  $N_r$ ) and carrying a step-by-step integration (using Kutta's Simpson's rule) of the differential Equations 2.1 along the whole plate. By enforcing the boundary conditions at the support:

$$w(r = b) = 0$$

and at the edge,

$$M_r(r = a) = 0$$



$$N_r(r = a) = 0$$

The Newton-Raphson scheme yields a set of corrected values for the assumed ones at the center of the plate. With these corrected values the procedure is repeated, and within a few iterations the solution of the problem will be determined.

The field variables at the center of the plate, the support, and the edge of the plate are denoted by subscripts 1, 2, and 3, respectively (Figure 4.1).

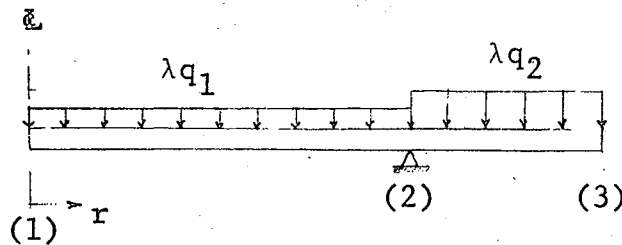


Figure 4.1. Section of the plate showing the boundaries.

Recall from the boundary conditions in Chapter 3 that  $u_1 = 0 = \phi_1$  for all possible loadings. Hence, we can treat the field variables  $u$ ,  $\phi$ ,  $w$ ,  $M_r$  and  $N_r$  as functions of  $r$ ,  $w_1$ ,  $M_{r_1}$  and  $N_{r_1}$  with  $\lambda$  as the load parameter.

The following relations may be written:

$$u = u(r, w_1, M_{r_1}, N_{r_1}; \lambda) \quad (4.12)$$

$$\phi = \phi(r, w_1, M_{r_1}, N_{r_1}; \lambda) \quad (4.1b)$$

$$w = w(r, w_1, M_{r_1}, N_{r_1}; \lambda) \quad (4.1c)$$

$$M_r = M_r(r, w_1, M_{r_1}, N_{r_1}; \lambda) \quad (4.1d)$$

$$N_r = N_r(r, w_1, M_{r_1}, N_{r_1}; \lambda) \quad (4.1e)$$

Given the values for  $w_1$ ,  $M_{r_1}$ ,  $N_{r_1}$ , and  $\lambda$  one can generate numerical values for the field variables  $u$ ,  $\phi$ ,  $w$ ,  $M_r$ , and  $N_r$  by applying Kutta's-Simpson's forward integration scheme. Recalling the boundary conditions (Chapter 3) at the support and at the edge of the plate, one can write:

$$0 = w_2 = w(b, w_1, M_{r_1}, N_{r_1}; \lambda) \quad (4.2a)$$

$$0 = M_{r_3} = M_r(a, w_1, M_{r_1}, N_{r_1}; \lambda) \quad (4.2b)$$

$$0 = N_{r_3} = N_r(a, w_1, M_{r_1}, N_{r_1}; \lambda) \quad (4.2c)$$

If we let  $w_1^a$ ,  $M_{r_1}^a$ , and  $N_{r_1}^a$  be close approximations to  $w_1$ ,  $M_{r_1}$  and  $N_{r_1}$ , respectively, one can write:

$$w_2^a = w(b, w_1^a, M_{r_1}^a, N_{r_1}^a; \lambda) \quad (4.3a)$$

$$M_{r_3}^a = M_r(a, w_1^a, M_{r_1}^a, N_{r_1}^a; \lambda) \quad (4.3b)$$

$$N_{r_3}^a = N_r(a, w_1^a, M_{r_1}^a, N_{r_1}^a; \lambda) \quad (4.3c)$$

$w_2^a$ ,  $M_{r_3}^a$ , and  $N_{r_3}^a$  will not satisfy Equations 4.2, and the Newton-Raphson method is then employed to determine  $w_1$ ,  $M_{r_1}$ , and  $N_{r_1}$ , such that the boundary conditions prescribed at the support and the edge of the plate are satisfied.

This is done by first expanding  $w_2$ ,  $M_{r_3}$ , and  $N_{r_3}$  in Taylor's series about  $w_1^a$ ,  $M_{r_1}^a$ , and  $N_{r_1}^a$  and neglecting the higher-order terms.

$$-w_2^a = \left(\frac{\partial w}{\partial w_1}\right)_{r=b} \delta w + \left(\frac{\partial w}{\partial M_{r_1}}\right)_{r=b} \delta M_r + \left(\frac{\partial w}{\partial N_{r_1}}\right)_{r=b} \delta N_r \quad (4.4a)$$

$$-M_{r_3}^a = \left(\frac{\partial M_r}{\partial w_1}\right)_{r=a} \delta w + \left(\frac{\partial M_r}{\partial M_{r_1}}\right)_{r=a} \delta M_r + \left(\frac{\partial M_r}{\partial N_{r_1}}\right)_{r=a} \delta N_r \quad (4.4b)$$

$$-N_{r_3}^a = \left(\frac{\partial N_r}{\partial w_1}\right)_{r=a} \delta w + \left(\frac{\partial N_r}{\partial M_{r_1}}\right)_{r=a} \delta M_r + \left(\frac{\partial N_r}{\partial N_{r_1}}\right)_{r=a} \delta N_r \quad (4.4c)$$

Having integrated Equations 2.1 along with the equations for the partial differential coefficients in Equations 4.4, which will be discussed later in this chapter, one can solve Equation 4.4 for  $\delta w$ ,  $\delta M_r$  and  $\delta N_r$ . This will yield improved approximations for  $w_1$ ,  $M_{r_1}$ , and  $N_{r_1}$  given by:

$$w_1^{a+1} = w_1^a + \delta w \quad (4.5a)$$

$$M_{r_1}^{a+1} = M_{r_1}^a + \delta M_r \quad (4.5b)$$

$$N_{r_1}^{a+1} = N_{r_1}^a + \delta N_r \quad (4.5c)$$

The procedure is repeated until convergence is reached.

There are two key steps for the implementation of the Newton-Raphson procedure: (1) determination of the partials; and (2) determination of an appropriate set of approximate values for  $w_1$ ,  $M_{r_1}$ , and  $N_{r_1}$ .

#### Determination of the Partials

Define:

$$(\quad)_i = \frac{\partial}{\partial i} (\quad),$$

where  $i$  may be either  $w_1$ ,  $M_{r_1}$ , or  $N_{r_1}$ .

By taking the partials of Equation 2.1 with respect to  $i$ , we derive the equations:

$$\frac{du_i}{dr} = \frac{1}{Eh} (N_{r_i} - \nu N_{t_i}) - \Phi \Phi_i \quad (4.6a)$$

$$\frac{d(r\Phi)_i}{dr} = \frac{r}{(1+\nu)D} (M_{r_i} + M_{t_i}) \quad (4.6b)$$

$$\frac{dw_i}{dr} = -\Phi_i \quad (4.6c)$$

$$\frac{d(rM_r)_i}{dr} = M_{t_i} - Q_i r \quad (4.6d)$$

$$\frac{d}{dr} (rN_r)_i = N_{t_i} \quad (4.6e)$$

$$N_{t_i} = Eh \frac{u_i}{r} + \nu N_{r_i} \quad (4.6f)$$

$$M_{t_i} = \nu M_{r_i} + (1 - \nu^2) D \frac{\phi_i}{r} \quad (4.6g)$$

$$Q_i = -N_r \phi_i - N_r \phi_i \quad (4.6h)$$

From previous discussion we observe that  $u_i$ ,  $\phi_i$ ,  $w_i$ ,  $M_{r_i}$ , and  $N_{r_i}$  are functions of  $w_1$ ,  $M_{r_1}$ ,  $N_{r_1}$  and also functions of  $(u_i)_1$ ,  $(\phi_i)_1$ ,  $(w_i)_1$ ,  $(M_{r_i})_1$ , and  $(N_{r_i})_1$ , with  $\lambda$ .

At  $r = 0$ :

$$u_i = \phi_i = 0 \quad \text{for } i = w_1, M_{r_1}, \text{ or } N_{r_1}$$

$$w_i = \begin{cases} 0 & \text{for } i = M_{r_1} \text{ or } N_{r_1} \\ 1 & \text{for } i = w_i \end{cases}$$

$$M_{r_i} = \begin{cases} 0 & \text{for } i = w_1 \text{ or } N_{r_1} \\ 1 & \text{for } i = M_{r_i} \end{cases}$$

$$N_{r_i} = \begin{cases} 0 & \text{for } i = w_1 \text{ or } M_{r_1} \\ 1 & \text{for } i = N_{r_i} \end{cases}$$

We now proceed and integrate Equations 4.6 using Kutta's-Simpson's rule of forward integration.

Determination of Good Estimates  
for  $w_1$ ,  $M_{r1}$ , and  $N_{r1}$

Suppose that for some particular value of the load parameter<sup>1</sup>  $\lambda$ , the solution was obtained. By now giving  $\lambda$  a small but otherwise arbitrary increment  $\Delta\lambda$  Equations 2.1 and 4.6 can now be integrated using the values of  $w_1$ ,  $M_{r1}$ , and  $N_{r1}$  determined at  $\lambda$ . The corresponding values that were obtained at positions 1, 2, and 3 (see Figure 4.1) would not satisfy the boundary conditions (i.e.,  $w_2 = M_{r3} = N_{r3} = 0$ ). Newton-Raphson root-finding scheme could then be employed to obtain an appropriate set of approximate values for  $w_1$ ,  $M_{r1}$ , and  $N_{r1}$  necessary for solving the plate problem at the new load.

---

1. The procedure is started by assigning a zero value to  $\lambda$ . The plate is then in the undeformed state. Hence the solution is known and the corresponding values of  $w_1$ ,  $M_{r1}$ , and  $N_{r1}$ , which are all zero, can be used as close estimates at the incremented load. Similarly, after the solution at this incremented load has been reached the corresponding values of  $w_1$ ,  $M_{r1}$ , and  $N_{r1}$  will then be treated as close estimates at a further incremented load, and so on.

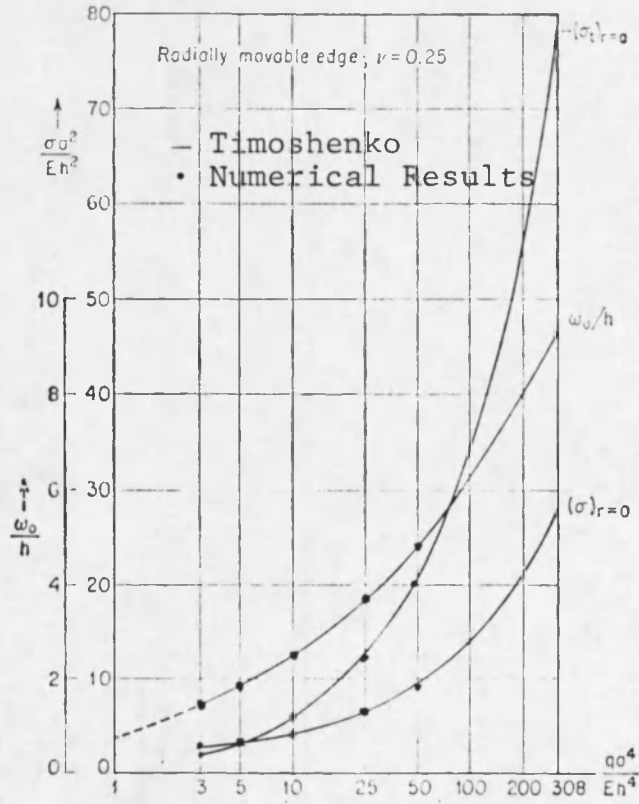
## CHAPTER 5

### PRESENTATION AND DISCUSSION OF RESULTS

Two numerical techniques were adopted in this research to solve the circular plate problem, namely the Newton-Raphson root-finding method and Kutta's-Simpson's rule of integration.

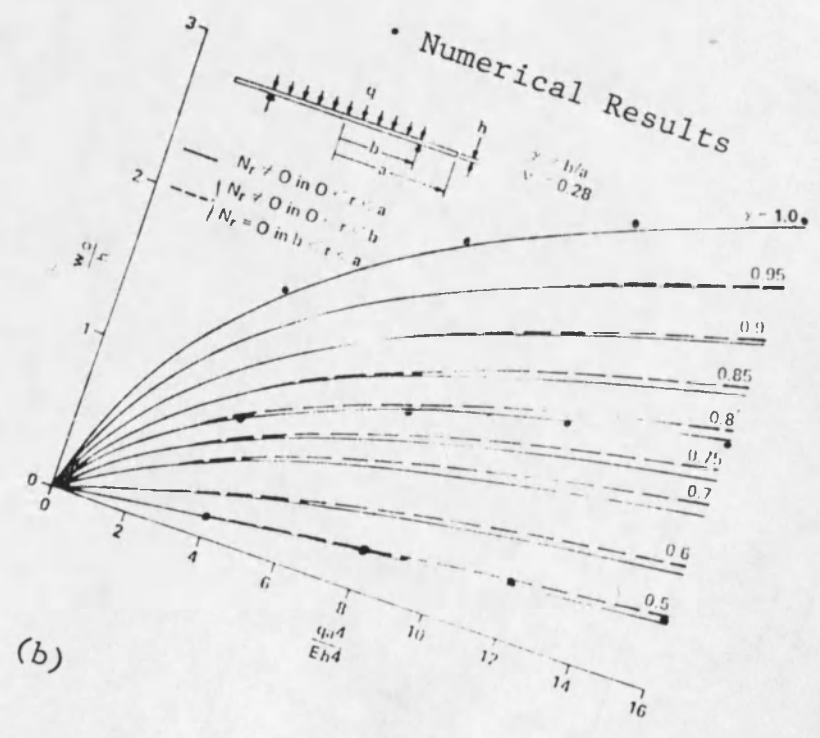
Kutta's-Simpson's rule of integrating the governing differential equations (2.1) could be employed by starting at any point along the plate.

In this study two cases were considered. First, the center of the plate was chosen and then the edge of the plate. Both yielded fairly accurate results which agreed very well with two special cases that have been considered in previous works. These cases were a circular plate supported at the edge by Timoshenko and Woinowsky-Krieger (1959), and a circular plate with an overhang by Lee et al. (1980) (Figure 5.1). However, when the center of the plate was first chosen, a small jump in the value of the radial moment occurred at the center, but this problem was eliminated when the edge of the plate was chosen. (Note: When the edge of the plate was chosen as the starting point, the field variables were then considered as



(a)





functions of  $r$  and the values of  $u$ ,  $\Phi$ , and  $w$  at the edge with  $\lambda$ .) The jump could be attributed to the singularity of the problem at the center of the plate. This is due to the fact that most of the governing differential equations involve a division by the radius, in particular near the center where the radius assumes a relatively small value.

Some results were obtained for a circular plate uniformly loaded within the support circle, for various ratios of edge-to-support radii and also for two different values of Poisson's ratio. These results are displayed in Figures 5.2 and 5.3. In Figure 5.2 the deflection at the center to the thickness of the plate ratio was plotted versus the non-dimensionalized load parameter  $q_1 a^4 / Eh^4$ . In Figure 5.3 the maximum tensile and compressive stresses at the center and at the edge, respectively, are plotted in a non-dimensionalized form  $\sigma a^2 / Eh^2$  versus  $q_1 a^4 / Eh^4$ .

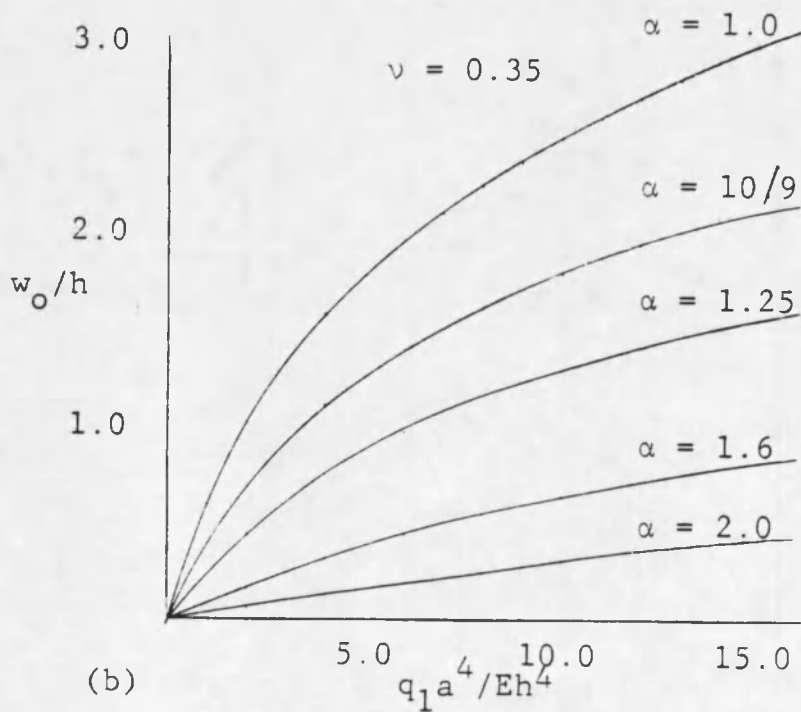
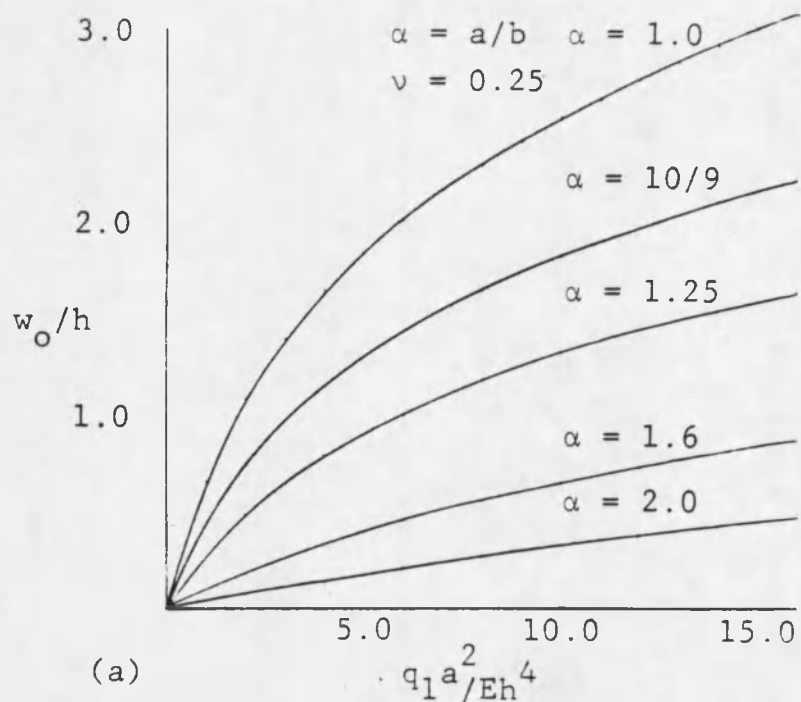


Figure 5.2. The deflection at the center of the plate versus the load, for different values of  $\alpha$ . -- (a)  $\nu = 0.25$ ; (b)  $\nu = 0.35$ .

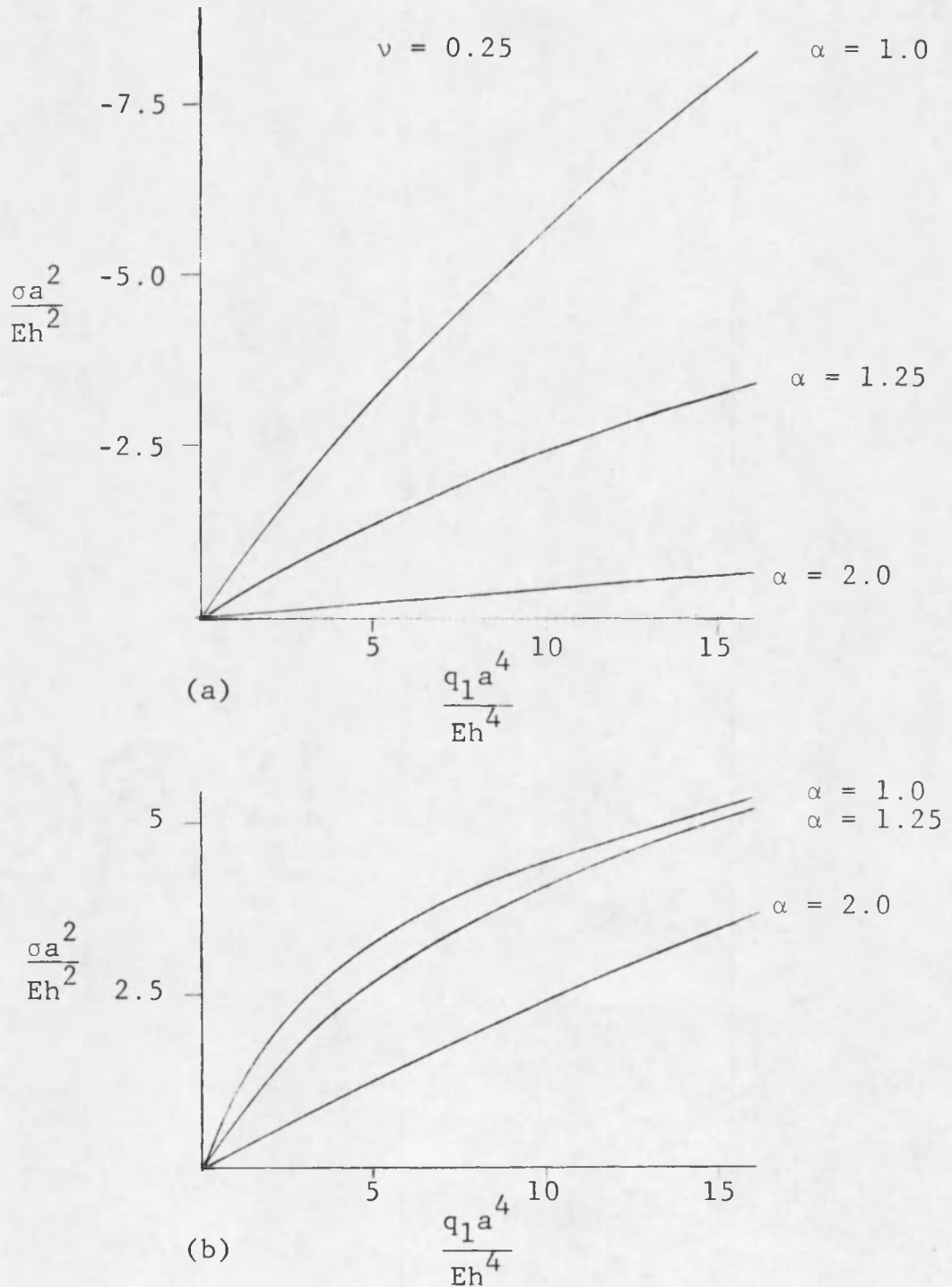


Figure 5.3. Stress versus load. -- (a) The compressive tangential stress at the edge, in the outer fiber; (b) The tensile stress at the center, in the outer fiber.

## CHAPTER 6

### CONCLUSION

It was demonstrated in the Lee et al. (1980) paper that the perturbation method that was employed in their research was more advantageous than the finite element approach. The latter could only obtain results for a specific problem with specific dimensions, whereas the perturbation technique could provide specific expressions whereby the deflections and stresses could be obtained for a large number of dimensions and loadings.

While the Lee et al. (1980) paper provided fairly accurate results, it was limited to solving circular plates uniformly loaded within the support circle. In this research, however, the plate could be loaded uniformly within the support circle, along the overhang, or any combination of the two, and accurate results were achieved.

## REFERENCES

Lee, H. C., C. K. Lim and H. D. Conway, "The Large Deflection of Thin Plates with Overhang," Journal of the Society for Experimental Stress Analysis, Experimental Mechanics, Vol. 20, No. 10, pp. 365-368, October 1980.

Timoshenko, S. and S. Woinowsky-Krieger, Theory of Plates and Shells, McGraw-Hill Book Company, 1959, Chapter 13.